Control Parameters Design of Spacecraft Formation Flying via Modified Biogeography-Based Optimization

Tianfu Chen[a], Dexin Zhang[b], Xiaowei Shao[c,*]

School of Aeronautics and Astronautics, Shanghai Jiao Tong University, Shanghai 200240, China

[a]chentianfu@sjtu.edu.cn, [b]dx_zhang@sjtu.edu.cn, [c]shaoxwmail@163.com

Abstract:
For spacecraft formation flying (SFF) missions, the effective control of relative motion is a critical issue. This paper investigates the problem of feedback parameters design in the trajectory tracking controller of SFF. To overcome the difficulty in manual parameters adjustment, a modified biogeography-based optimization (M-BBO) algorithm is employed by transforming the parameters tuning into an optimization problem. In the proposed M-BBO, the new component is a hybrid operator, where the search mechanism of grasshopper optimization algorithm is integrated into the migration operation of biogeography-based optimization (BBO). It helps M-BBO achieve a better balance between exploitation and exploration abilities, thereby facilitating the generation of promising candidate solutions. During the optimization process, the objective function is a weighted sum that considers the tracking error and fuel consumption of the SFF controller. Simulation results show that the parameters obtained via M-BBO ensure the accurate control at low cost, and comparative experiments with other versions of BBO are conducted to prove the M-BBO's superiority in terms of convergence performance.

Keywords: Spacecraft formation flying; Control parameters optimization; Biogeography-based optimization

1. Introduction

Spacecraft formation flying (SFF) is a significant technology for certain space missions [1]. With notable merits such as low cost, high efficiency and great flexibility, SFF expands the functions of traditional single spacecraft. To guarantee the practical implementation of SFF, it is required to perform valid control of relative position between spacecraft [2].

One major goal of SFF control is that the spacecraft can track a desired relative trajectory, and extensive researches have focused on the design of SFF controller. Some popular techniques of SFF control included linear quadratic control, model predictive control and slide mode control [3-5]. To obtain expected control performance, the controller parameters commonly need to be identified through the designers' experience, which is a challenging task in the control system [6].

Recently, owing to automating the parameter adjustment, the application of bio-inspired optimization algorithms to control parameters design has attracted much attention. Steinberg and Page [7] developed a backstepping control scheme with parameter optimization done by a genetic algorithm (GA), which was favorable for the multi-axis control of a high-performance aircraft. In [8], the GA was also employed to optimally search the control gains of pitch autopilot for aircraft landing. Lu et al. [9] suggested a control strategy of turbine engine based on particle swarm optimization (PSO), where proportional-integral-differential parameters are tuned via PSO. Additionally, Zhang and An [10] provided an intelligent methodology using PSO for gain scheduling controllers and thus facilitated the automation of flight control design. Deng and Duan [11] optimized the selection of control parameters in the carrier landing system by pigeon-inspired optimization (PIO). Aiming at satellite formation keeping, Soyinka and Duan [12] regarded mean orbit elements as feedback and proposed the chaotic artificial bee colony (ABC) algorithm to estimate the feedback gain. It can be seen that combining the bio-inspired approaches with the controller design works well in a number of studies.

When it comes to the emerging bio-inspired methods for global optimization, biogeography-based optimization (BBO) cannot be underestimated because it has demonstrated remarkable success in diverse engineering cases [13-15]. BBO is modeled after the distribution mechanism of

* Corresponding author.

biological species among habitats. Similar to many evolutionary algorithms (EAs), BBO enables candidate solutions to share information with each other. In BBO, the solutions change probabilistically by the migration operation, which distinguishes BBO from reproductive manners like GA. Moreover, for each solution, the migration rate is governed by its quality. It is these features that make BBO become a powerful optimization tool [13]. Generally, BBO has an excellent exploitation ability, which triggers the hybridization of BBO with other EAs that are good at exploration. For instance, the mutation operator of differential evolution (DE) was merged with BBO to increase the population diversity while preserving the exploitation [16].

In this study, a modified BBO (M-BBO) method is presented to enhance the balance in BBO between exploitation and exploration. The strategy of updating the solutions in grasshopper optimization algorithm (GOA) [17] is introduced into the standard BBO migration operation. According to [17], GOA is able to explore the search space well, and this is the motivation of redesigning the migration operator. Then, M-BBO is applied to adjust the controller parameters of SFF along elliptical orbits. By feeding back the errors of relative position and velocity, a nonlinear control law based on Lyapunov theory is achieved. The fitness function evaluated during the optimization is a linear weighted cost function, in which tracking accuracy and fuel consumption are taken into account simultaneously. The contribution of this paper is twofold. First, the task of acquiring parameters in the SFF controller is converted to an optimization problem, and BBO is considered as a solver. Second, M-BBO that assimilates the advantage of GOA is proposed, where a new migration operator integrates the exploitation of BBO and the exploration of GOA.

The rest of this paper is as follows. The relative translational dynamics and controller design of SFF are described in Section 2. The basic BBO and its modified version are contained in Section 3. The detailed implementation of M-BBO for control parameters optimization is presented in Section 4, followed by numerical simulations and experimental results in Section 5. Finally, Section 6 concludes the paper.

2. System Model of SFF

2.1 Relative-motion dynamics

Consider a SFF system consisting of two spacecraft, namely, the leader and follower, as shown in Fig. 1. Let $I=\{X_i,Y_i,Z_i\}$ denote the Earth-centered inertial (ECI) frame, and $\boldsymbol{r}_l$ mean the position vector from the center of Earth to the leader. The motion of the follower relative to the leader is modeled in the local-vertical-local-horizontal (LVLH) frame $L=\{X_l,Y_l,Z_l\}$, whose origin is located at the mass center of the leader. The X_l axis points in the direction of $\boldsymbol{r}_l$, the Z_l axis is along the angular momentum vector of the leader and the Y_l axis completes the right-handed orthogonal coordinate system.

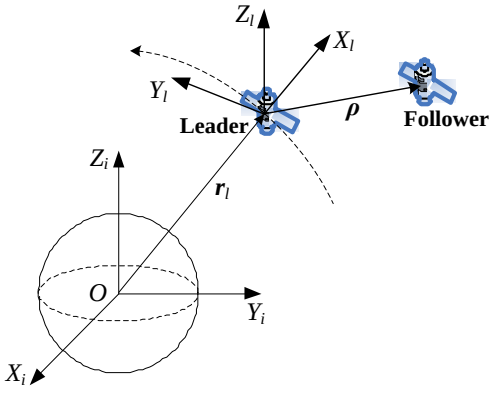

Fig. 1. Schematic diagram of SFF system.

The relative dynamics between the leader and follower [18] can be formulated as

$$\ddot{\boldsymbol{\rho}}+\boldsymbol{C}(\omega_l)\dot{\boldsymbol{\rho}}+\boldsymbol{N}(\boldsymbol{\rho},\boldsymbol{r}_l,\omega_l,\dot{\omega}_l)=\boldsymbol{D}+\boldsymbol{u} \tag{1}$$

where $\boldsymbol{\rho}=\begin{bmatrix} x & y & z \end{bmatrix}^T$ is the relative position in the LVLH frame and $r_l=\|\boldsymbol{r}_l\|=\dfrac{a\left(1-e^2\right)}{1+e\cos\theta}$; a, e and θ are the semi-major axis, the eccentricity and the true anomaly of the leader orbit, respectively; $\boldsymbol{D}$ is the relative disturbance vector and $\boldsymbol{u}$ is the control input. The leader's orbital angular velocity ω_l and angular acceleration $\dot{\omega}_l$ are given as follows:

$$\omega_l=\dot{\theta}=\frac{\sqrt{\mu a\left(1-e^2\right)}}{r_l^2},\ \dot{\omega}_l=\ddot{\theta}=-\frac{2\mu e\sin\theta}{r_l^3} \tag{2}$$

where μ is the gravitational constant of Earth. The skew-symmetric matrix $\boldsymbol{C}(\bullet)$ is written as

$$\boldsymbol{C}\left(\omega_l\right)=2\omega_l\begin{bmatrix} 0 & -1 & 0 \\ 1 & 0 & 0 \\ 0 & 0 & 0 \end{bmatrix} \tag{3}$$

The nonlinear term $\boldsymbol{N}(\bullet)$ is expressed as

$$\boldsymbol{N}\left(\boldsymbol{\rho},\boldsymbol{r}_l,\omega_l,\dot{\omega}_l\right)=\begin{bmatrix} \mu\left(\dfrac{r_l+x}{\|\boldsymbol{r}_l+\boldsymbol{\rho}\|^3}-\dfrac{1}{r_l^2}\right)-\omega_l^2x-\dot{\omega}_l y \\ \left(\dfrac{\mu}{\|\boldsymbol{r}_l+\boldsymbol{\rho}\|^3}-\omega_l^2\right)y+\dot{\omega}_l x \\ \dfrac{\mu}{\|\boldsymbol{r}_l+\boldsymbol{\rho}\|^3}z \end{bmatrix} \tag{4}$$

2.2 Lyapunov-based control

Given a reference trajectory $\boldsymbol{\rho}_d=\begin{bmatrix} x_d & y_d & z_d \end{bmatrix}^T$ of the follower relative to the leader, then the position tracking error can be computed as $\boldsymbol{e}=\boldsymbol{\rho}-\boldsymbol{\rho}_d$. Using the error vector and its time derivative, the control Lyapunov function is defined as

$$V\left(\boldsymbol{e},\dot{\boldsymbol{e}}\right)=\frac{1}{2}\boldsymbol{e}^T\boldsymbol{K}_1\boldsymbol{e}+\frac{1}{2}\dot{\boldsymbol{e}}^T\dot{\boldsymbol{e}} \tag{5}$$

where $\boldsymbol{K}_1\in R^{3\times3}$ is a positive definite position feedback gain matrix. Taking the time derivative of Eq. (5) leads to

$$\dot{V}=\dot{\boldsymbol{e}}^T\left(\boldsymbol{K}_1\boldsymbol{e}+\ddot{\boldsymbol{\rho}}-\ddot{\boldsymbol{\rho}}_d\right) \tag{6}$$

Setting $\boldsymbol{D}=0$ in Eq. (1) and substituting Eq. (1) into Eq. (6) yields

$$\dot{V}=\dot{\boldsymbol{e}}^T\left(\boldsymbol{K}_1\boldsymbol{e}-\boldsymbol{C}(\bullet)\dot{\boldsymbol{\rho}}-\boldsymbol{N}(\bullet)+\boldsymbol{u}-\ddot{\boldsymbol{\rho}}_d\right) \tag{7}$$

Enforcing $\dot{V}$ to be the negative quantity

$$\dot{V}=-\dot{\boldsymbol{e}}^T\boldsymbol{K}_2\dot{\boldsymbol{e}} \tag{8}$$

where $\boldsymbol{K}_2\in R^{3\times3}$ is a positive definite velocity feedback gain matrix, the control law [19] can be deduced as

$$\boldsymbol{u}=-\boldsymbol{K}_1\boldsymbol{e}-\boldsymbol{K}_2\dot{\boldsymbol{e}}+\boldsymbol{C}(\bullet)\dot{\boldsymbol{\rho}}+\boldsymbol{N}(\bullet)+\ddot{\boldsymbol{\rho}}_d \tag{9}$$

When $\dot{V}=0$ (i.e., $\dot{\boldsymbol{e}}=\boldsymbol{0}$), the second and third derivatives of V with respect to time are

$$\begin{cases} \dot{V}=0 \\ \ddot{V}=-2\boldsymbol{e}^T\boldsymbol{K}_1^T\boldsymbol{K}_2\boldsymbol{K}_1\boldsymbol{e}<0,\ \forall\boldsymbol{e}\neq\boldsymbol{0} \end{cases} \tag{10}$$

From the stability theorem in [20], Eq. (10) can indicate that the closed loop system with the control law $\boldsymbol{u}$ is asymptotically stable.

3. M-BBO algorithm

3.1 Principles of the basic BBO

In natural biogeography, the extent to which a habitat is suitable for living is judged by the habitat suitability index (HSI). Numerous factors can exert influences on the HSI, and they are collectively called the suitability index variables (SIVs). As a population-based algorithm, BBO treats each candidate solution as a habitat. The goodness of one individual is measured by HSI, and each component of the individual is analogous to a SIV.

Migration, one core operator of BBO, makes the best use of feature sharing among the individuals. In BBO, a good individual stands for a high-HSI habitat which has relatively low immigration rate (λ) and high emigration rate (φ), while the converse is true for an inferior individual. For the *k*th individual H_k in the population, according to the linear migration model in [13], the migration rates are represented as follows:

$$\gamma_k = I\left(1-\frac{r(k)}{N_{\mathrm{P}}}\right), \varphi_k = E\frac{r(k)}{N_{\mathrm{P}}} \tag{11}$$

where N_{P} is the population size and $r(k)$ is the HSI rank of H_k (1 is the worst and N_{P} is the best); I is the maximum immigration rate and E is the maximum emigration rate. Under the migration mechanism, the probability that H_k is chosen for immigration is proportional to γ_k. Subsequently, the emigrating habitat H_j is pick via roulette wheel selection based on all the φ values of the population. The migration equation can be formulated as

$$H_k(\mathrm{SIV}) = H_j(\mathrm{SIV}) \tag{12}$$

Notice that the good solutions are more likely to pass on their own features to others, while the poor solutions are inclined to accept new information from others.

The HSI of a habitat can be dramatically changed due to cataclysmic events, and this phenomenon is modeled as SIV mutation in BBO. The relationship between mutation rate σ_k and species count probability P_k is expressed as

$$\sigma_k = \sigma_{\max}\left(1-\frac{P_k}{P_{\max}}\right) \tag{13}$$

where $\sigma_{\max}$ is the maximum mutation rate and $P_{\max} = \max P_k, k = 1,2,...,N_{\mathrm{P}}$. For details on the calculation of P_k, see [21]. The mutation operator makes both high-HSI and low-HSI solutions have the chance to mutate, thereby promoting the diversity among the population.

3.2 New migration operator of M-BBO

As mentioned above, in the migration process, the solution features of good individuals might substitute certain features of poor individuals. The acquisition of new features can upgrade these poor individuals, which means that BBO exploits the information of the current population finely. On the other hand, the existence of these features in both good and poor individuals results in the lack of population diversity and exploration capacity. It is worth pointing out that exploitation and exploration are mutually contradictory, and the two abilities should be well counterpoised so that BBO can possess better optimization performance.

The new operator of M-BBO is a hybrid migration operator, which involves the original migration operator of BBO and the position-updating operator of GOA. GOA is a novel intelligent optimization method and simulates the swarming behavior of grasshoppers. The movement of grasshoppers in nature is mainly affected by social interaction, gravity force and windy advection. In GOA, to settle optimization problems effectively, gravity force is neglected and the wind

direction is assumed to be towards the grasshopper with the best fitness. Suppose the *d*-dimensional position of the individual (grasshopper) H_k in the *l*th iteration is $H_k^d(l)$. The mathematical model is built as follows to update the status of the next iteration [17]:

$$H_k^d(l+1) = c\left(\sum_{\substack{j=1 \\ j\neq k}}^{N_P} c\frac{ub_d - lb_d}{2} S(|\Delta r|)\frac{\Delta r}{d_{jk}}\right) + H_{\text{best}}^d(l) \tag{14}$$

$$S(r) = \alpha e^{-\frac{r}{\beta}} - e^{-r} \tag{15}$$

$$\Delta r = H_j^d(l) - H_k^d(l) \tag{16}$$

where ub_d and lb_d are the upper and lower bound of the *d*th dimension, respectively; H_{best}^d is the value of the *d*th dimension in the best individual found so far; d_{jk} is the distance between the individuals H_j and H_k. The function S defines the strength of social forces, α in S stands for the intensity of attraction, and β in S is the attractive length scale. α and β typically equal to 0.5 and 1.5. c is a parameter that impacts on the exploitation and exploration in GOA. A large c indicates that the dominant activity of GOA is exploration; a small c indicates that the dominant activity is exploitation. It should be noted that c is set as 1 in this study to fully utilize the exploration potential of GOA.

```
1. for k = 1 to N_P do
2.     for d = 1 to D do
3.         if rand < γ_k then
4.             for j = 1 to N_P do
5.                 Select H_j with probability ∝ φ_j
6.                 if H_j is selected then
7.                     H_k^d ← H_j^d
8.                 end if
9.             end for
10.        else
11.            Update H_k^d by Eqs. (14)-(16)
12.            Bring the current individual back if it goes outside the bounds
13.        end if
14.    end for
15. end for
```

Fig. 2. Algorithm for new migration operator in M-BBO.

In M-BBO, a new migration operator is proposed, where the position-updating mode of GOA is incorporated into the BBO's migration framework, as illustrated in Fig. 2. In Fig. 2, D is the dimension of decision space, and *rand* is a function generating a random number uniformly distributed in $(0,1)$. The new operator unites the advantages of BBO and GOA as much as possible. Each dimension of H_k has a probability of γ_k to employ the original migration, which maintains the outstanding property concerning the local searching ability in BBO. Meanwhile, each dimension of H_k has a probability of $(1-\gamma_k)$ to update in the evolutionary way of GOA. From Eq. (14), the next position of an individual is decided by its current position, the global best, and the position of all other individuals. This is beneficial to searching globally and increasing the diversity of search space. Hence, M-BBO could exhibit the reasonable trade-off between exploitation and exploration.

4. Control parameters design based on M-BBO

4.1 Problem formulation

In the Lyapunov-based SFF controller derived in Section 2.2, the parameters of the matrices $\boldsymbol{K}_1$ and $\boldsymbol{K}_2$ are conventionally regulated by cut-and-try method, which usually calls for plenty

of experience and tests. To alleviate the workload of designers and achieve optimal control characteristic, this study looks on the parameters identification of SFF controller as a continuous-domain optimization problem.

Let $\boldsymbol{K}_1$ and $\boldsymbol{K}_2$ be diagonal matrices for simplicity, then they can be written as

$$\boldsymbol{K}_1 = \begin{bmatrix} K_{1,1} & 0 & 0 \\ 0 & K_{1,2} & 0 \\ 0 & 0 & K_{1,3} \end{bmatrix}, \boldsymbol{K}_2 = \begin{bmatrix} K_{2,1} & 0 & 0 \\ 0 & K_{2,2} & 0 \\ 0 & 0 & K_{2,3} \end{bmatrix} \tag{17}$$

where all the diagonal elements are positive. In view of this, there are six control parameters to be optimized in the decision vector $\boldsymbol{X} = \begin{bmatrix} K_{1,1} & K_{1,2} & K_{1,3} & K_{2,1} & K_{2,2} & K_{2,3} \end{bmatrix}^T$.

The control objective is that the bounded motion of SFF and low fuel cost can be ensured. Therefore, two fitness functions are defined for the optimization problem. The first function intends to lessen the tracking error between the actual and desired trajectory, and it can be calculated as

$$f_1 = \int_0^{t_f} \left\| \boldsymbol{\rho}(t) - \boldsymbol{\rho}_d(t) \right\| dt \tag{18}$$

where t_f is the total duration. The second function denotes the fuel cost during the control process, the expression of which is

$$f_2 = \int_0^{t_f} \left| u_x(t) \right| + \left| u_y(t) \right| + \left| u_z(t) \right| dt \tag{19}$$

where $u_m \left(m = x, y, z \right)$ is the component of the control acceleration $\boldsymbol{u}$.

The mathematical model of control parameters optimization is formulated as

$$\begin{aligned} &\min_{\boldsymbol{X}} F(\boldsymbol{X}) = \omega_1 f_1 + \omega_2 f_2 \\ &\text{s.t. } \boldsymbol{X} \in R^{6\times 1} : X_j^l < X_j < X_j^u \left(j = 1,2,3,4,5,6 \right) \end{aligned} \tag{20}$$

where ω_1 and ω_2 are the weight coefficients, reflecting the importance of the fitness functions; X_j^l and X_j^u are the lower and upper bound of the corresponding decision variable in $\boldsymbol{X}$.

4.2 Implementation procedure of M-BBO for parameters optimization

The proposed M-BBO is used to handle the single-objective optimization model in Eq. (20). The procedure of M-BBO for attaining the control parameters in SFF is described as follows:

Step 1 Input the orbital elements of the leader, the initial position $\boldsymbol{\rho}_0$ and desired trajectory $\boldsymbol{\rho}_d$ of the follower in the LVLH frame, the total control time t_f, the weights ω_1 and ω_2, the search ranges of decision variables $\left(X_j^l, X_j^u \right)$ and the parameters in M-BBO (including population size N_{P}, maximum optimization generation N_{G}, maximum migration rates I and E, maximum mutation rate $\sigma_{\max}$).

Step 2 Generate an initial population and initialize generation number $n_{\mathrm{G}} = 0$.

Step 3 Evaluate the weighted optimization objective value in Eq. (20) for each individual in the population.

Step 4 Apply elitism mechanism: updating the best solution H_{best}, which will replace the worst solution of the current population if H_{best} does not exist in the present generation.

Step 5 If the maximum generation number is reached ($n_{\mathrm{G}} \geq N_{\mathrm{G}}$), output the optimal control parameters. Otherwise, go to step 6.

Step 6 Compute the immigration rates, emigration rates and mutation rates according to the ranking result of the fitness.

Step 7 Perform the new migration operator as discussed in Section 3.2.

Step 8 Conduct the mutation operator as discussed in Section 3.1.

Step 9 Update the generation number $n_G = n_G + 1$ and go to step 3 for the next iteration.

The flow diagram of control parameters design based on M-BBO is also outlined in Fig. 3.

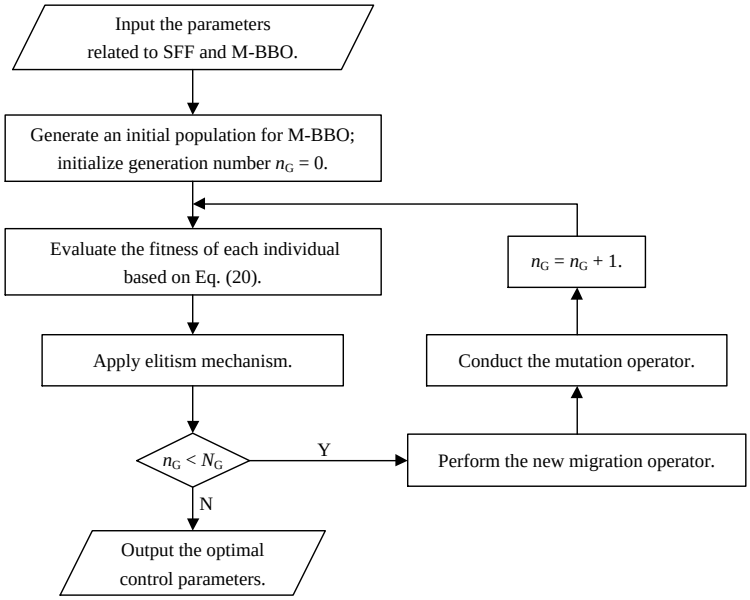

Fig. 3. Flow chart of M-BBO for SFF control parameters optimization.

5. Simulation

To validate the effectiveness of the developed strategy of using M-BBO to optimize the control parameters in SFF, an example of two-spacecraft formation is demonstrated. The leader is assumed to be perfectly controlled in an elliptical orbit with semi-major axis 6878.137km and eccentricity 0.1. The initial true anomaly of the leader is 0°. The follower has the initial values $\boldsymbol{\rho}_0 = [-100, 900, 150]^T$ m, and it ought to track the sinusoidal trajectories $\boldsymbol{\rho}_d = [500\sin(nt), 1000\cos(nt), 500\sqrt{3}\sin(nt)]^T$ m, where n is the mean angular velocity of the leader. The disturbances are assumed to be known, since these do not belong to the main scope of the present work. In this simulation, $\boldsymbol{D} = [2\sin(nt), 2\cos(nt), 2\sin(nt)]^T \times 10^{-5}\,\mathrm{m/s^2}$. The simulating time of the controller is set as $t_f = 2\pi/n$.

For the optimization model in Eq. (20), the weights are chosen as $\omega_1 = 1$ and $\omega_2 = 10^5$; the lower bounds of six decision variables are all considered as 0 and the upper bounds are set as $X_j^u = 2\times10^{-5}\ (j = 1,2,3)$ and $X_j^u = 2\times10^{-2}\ (j = 4,5,6)$. The relevant parameters of M-BBO are tabulated in Table 1. Fig. 4 depicts the convergence process, where the final value of fitness reaches 4.346×10^5. The optimized result of control parameters is displayed in Table 2.

Table 1. Simulation parameters of M-BBO algorithm.

Parameter	Value
Population size N_P	30
Maximum generation number N_G	25
Maximum immigration rate I	1
Maximum emigration rate E	1
Maximum mutation rate σ_{max}	0.01

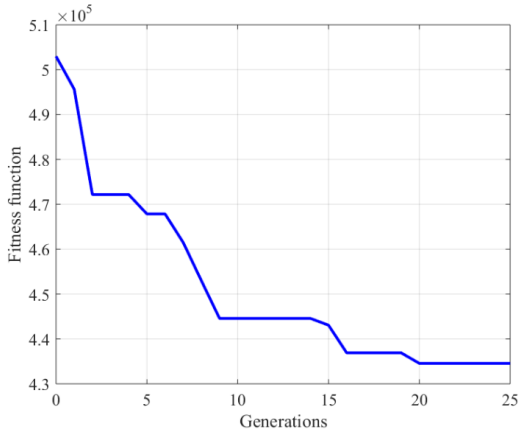

Fig. 4. Convergence process of M-BBO.

Table 2. Control parameters obtained by M-BBO algorithm.

Parameter	$K_{1,1}$	$K_{1,2}$	$K_{1,3}$	$K_{2,1}$	$K_{2,2}$	$K_{2,3}$
Value	1.842×10^{-5}	1.995×10^{-5}	1.640×10^{-5}	1.114×10^{-2}	9.282×10^{-3}	6.042×10^{-3}

Fig. 5 plots the follower's three-dimensional trajectories in the LVLH frame under the set of parameters in Table 2. The time histories of relative position error $\|\boldsymbol{e}(t)\|$ are shown in Fig. 6. As can be seen, the optimized controller based on M-BBO can support the accomplishment of the given mission for tracking the desired trajectory. Fig. 7 illustrates the time histories of total fuel consumption $\Delta V(t)$. At the time of t_f, the fuel cost of the control is 3.259m/s.

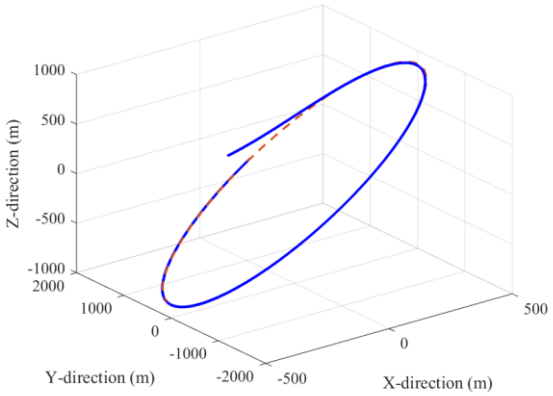

Fig. 5. Actual controlled trajectory (solid line) and desired trajectory (dashed line).

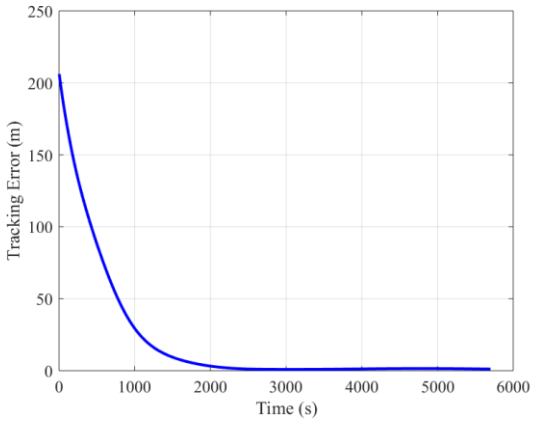

Fig. 6. Tracking error of the follower.

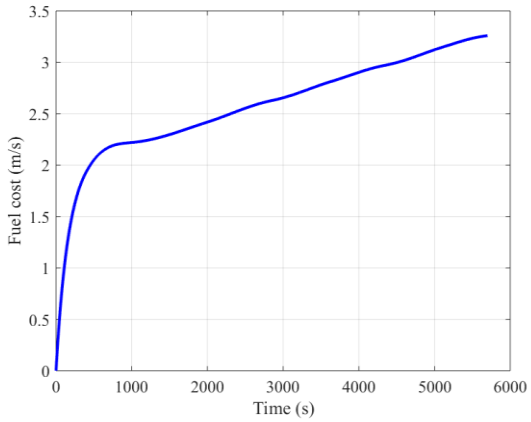

Fig. 7. Total fuel cost.

In order to testify the improvement of M-BBO for identifying the control parameters of SFF, the comparative experiments with the original BBO [13] and the blend BBO (B-BBO) [22] are carried out. Note that these optimization algorithms have the same initialization part, which evades the influence of different initializations. Some requisite parameters are consistent with those in Table 1. The evolution curves of three methods are depicted in Fig. 8. The convergence quality of M-BBO is better in contrast to the others, which reveals the assistance of new migration operator in the optimization process. This is because that the redesigned operator strengthens the exploration ability and prevents the population falling into the local optima in some degree.

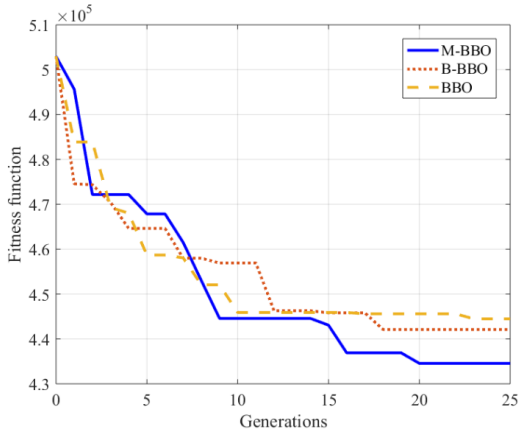

Fig. 8. Comparative convergence process of M-BBO with other optimizations.

Furthermore, 30 independent simulation runs of three algorithms for tuning the control parameters are conducted. Table 3 lists the best fitness value and the mean fitness value attained by each algorithm. It can be found that M-BBO outperforms the other two methods with regard to the best and average performance. The results here imply that M-BBO is at least competitive with BBO and B-BBO, and could be a valuable tool for designing the controller of SFF.

Table 3. Comparative results between three algorithms.

	BBO	B-BBO	M-BBO
Best minimum	4.420×10^5	4.409×10^5	4.337×10^5
Mean minimum	4.448×10^5	4.416×10^5	4.353×10^5

6. Conclusion

In this paper, the problem of optimizing the control parameters for SFF missions is addressed. A nonlinear Lyapunov-based control law is adopted, and the key of the optimization is tuning the feedback matrix parameters of the controller. A modified version of BBO, i.e., M-BBO, is presented to deal with this parameter optimization problem. By virtue of the new migration operator, which absorbs the exploration of GOA without destroying the exploitation of BBO, M-BBO has an appropriate balance between solution diversification and intensification. With the help

of M-BBO, the generated SFF controller can guarantee an excellent performance index that makes an overall evaluation on tracking error and fuel cost. Comparative results suggest that the proposed M-BBO is a feasible and superior method for determining the SFF control parameters.

The control parameters design in this paper considers a weighted fitness function and is only targeted at the single-objective optimization. In the future work, applying multi-objective optimization algorithms to the research field of SFF control is worthy of investigation.

References

[1] L.A. Sobiesiak, C.J. Damaren, Impulsive spacecraft formation maneuvers with optimal firing times, Journal of Guidance, Control, and Dynamics. 38 (10) (2015) 1994-1999.

[2] R. Sun, J. Wang, D. Zhang, et al., Roto-translational spacecraft formation control using aerodynamic forces, Journal of Guidance, Control, and Dynamics. 40 (10) (2017) 2556-2568.

[3] R. Kristiansen, P.J. Nicklasson, Spacecraft formation flying: A review and new results on state feedback control, Acta Astronautica. 65 (11-12) (2009) 1537-1552.

[4] Y. Lim, Y. Jung, H. Bang, Robust model predictive control for satellite formation keeping with eccentricity/inclination vector separation, Advances in Space Research. 61 (10) (2018) 2661-2672.

[5] H. Liu, J. Li, Terminal sliding mode control for spacecraft formation flying, IEEE Transactions on Aerospace and Electronic Systems. 45 (3) (2009) 835-846.

[6] Z. Yang, H. Duan, Y. Fan, et al., Automatic carrier landing system multilayer parameter design based on Cauchy mutation pigeon-inspired optimization, Aerospace Science and Technology. 79 (2018) 518-530.

[7] M.L. Steinberg, A.B. Page, Nonlinear adaptive flight control with genetic algorithm design optimization, International Journal of Robust and Nonlinear Control. 9 (14) (1999) 1097-1115.

[8] J.G. Juang, H.K. Chiou, L.H. Chien, Analysis and comparison of aircraft landing control using recurrent neural networks and genetic algorithms approaches, Neurocomputing. 71 (16-18) (2008) 3224-3238.

[9] J. Lu, C. Yang, B. Peng, et al., Self-tuning PID control scheme with swarm intelligence based on support vector machine, in: IEEE International Conference on Mechatronics and Automation, 2014, pp. 1554-1558.

[10] M. Zhang, J. An, Application of intelligent computation to promote the automation of flight control design, in: International Conference on Intelligent Computation Technology and Automation, 2008, pp. 991-994.

[11] Y. Deng, H. Duan, Control parameter design for automatic carrier landing system via pigeon-inspired optimization, Nonlinear Dynamics. 85 (1) (2016) 97-106.

[12] O.K. Soyinka, H. Duan, Satellite formation keeping via chaotic artificial bee colony, Aircraft Engineering and Aerospace Technology. 89 (2) (2017) 246-256.

[13] D. Simon, Biogeography-based optimization, IEEE Transactions on Evolutionary Computation. 12 (6) (2008) 702-713.

[14] V. Panchal, P. Singh, N. Kundra, et al., Biogeography based satellite image classification, International Journal of Computer Science and Information Security. 6 (2) (2009) 269-274.

[15] S.H.A. Rahmati, M. Zandieh, A new biogeography-based optimization (BBO) algorithm for the flexible job shop scheduling problem, The International Journal of Advanced Manufacturing Technology. 58 (9-12) (2012) 1115-1129.

[16] W. Gong, Z. Cai, C.X. Ling, DE/BBO: A hybrid differential evolution with biogeography-based optimization for global numerical optimization, Soft Computing. 15 (4) (2011) 645-665.

[17] S. Saremi, S. Mirjalili, A. Lewis, Grasshopper optimisation algorithm: theory and application, Advances in Engineering Software. 105 (2017) 30-47.

[18] A. Imani, M. Bahrami, Optimal sliding mode control for spacecraft formation flying in eccentric orbits, Proceedings of the Institution of Mechanical Engineers, Part I: Journal of Systems and Control Engineering. 227 (5) (2013) 474-481.

[19] Y. Zhang, Study on dynamics and control technology of satellite formation flying, Ph.D. dissertation, National University Defense Technology, 2002.

[20] R. Mukherjee, D. Chen, Asymptotic stability theorem for autonomus systems, Journal of Guidance, Control, and Dynamics. 16 (5) (1993) 961-963.

[21] H. Ma, An analysis of the equilibrium of migration models for biogeography-based optimization, Information Sciences. 180 (18) (2010) 3444-3464.

[22] H. Ma, D. Simon, Blended biogeography-based optimization for constrained optimization, Engineering Applications of Artificial Intelligence. 24 (3) (2011) 517-525.